2. B. Bosworth, K. Zhang, "Evidence of Increasing Differential Mortality: A Comparison of the HRS and SIPP," Center for Retirement Research at Boston College Working Paper 2015-13 (2015).
3. R. Chetty *et al.*, *JAMA* 10.1001/jama.2016.4226 (2016).
4. National Research Council, Committee on the Long-Run Macroeconomic Effects of the Aging U.S. Population, "The Growing Gap in Life Expectancy by Income: Implications for Federal Programs and Policy Responses" (2015).
5. J. Pijoan-Mas, J. V. Ríos-Rull, *Demography* **51**, 2075–2102 (2014).
6. H. Waldron, *Soc. Secur. Bull.* **67**, 1–28 (2007).
7. H. Waldron, *Soc. Secur. Bull.* **73**, 1–37 (2013).
8. J. Wilmoth, C. Boe, M. Barbieri, in *International Differences in Mortality at Older Ages: Dimensions and Sources*, E. M. Crimmins, S. H. Preston, B. Cohen, Eds. (National Academies Press, Washington, DC, 2011), pp. 337–372.
9. G. K. Singh, M. Siahpush, *Int. J. Epidemiol.* **35**, 969–979 (2006).
10. M. Ezzati, A. B. Friedman, S. C. Kulkarni, C. J. Murray, *PLOS Med.* **5**, e66 (2008).
11. C. J. Murray *et al.*, *PLOS Med.* **3**, e260 (2006).
12. H. Wang, A. E. Schumacher, C. E. Levitz, A. H. Mokdad, C. J. Murray, *Popul. Health Metr.* **11**, 8 (2013).
13. J. S. Olshansky *et al.*, *Health Aff.* **31**, 1803–1813 (2011).
14. E. R. Meara, S. Richards, D. M. Cutler, *Health Aff.* **27**, 350–360 (2008).
15. D. M. Cutler, F. Lange, E. Meara, S. Richards-Shubik, C. J. Ruhm, *J. Health Econ.* **30**, 1174–1187 (2011).
16. J. K. Montez, L. F. Berkman, *Am. J. Public Health* **104**, e82–e90 (2014).
17. Human Mortality Database; www.mortality.org.
18. D. D. Reidpath, P. Allotey, *J. Epidemiol. Community Health* **57**, 344–346 (2003).
19. A. Case, A. Deaton, *Proc. Natl. Acad. Sci. U.S.A.* **112**, 15078–15083 (2015).
20. J. Bound, A. Geronimus, J. Rodriguez, T. Waidman, "The Implications of Differential Trends in Mortality for Social Security Policy," University of Michigan Retirement Research Center Working Paper 2014-314 (2014).
21. J. B. Dowd, A. Hamoudi, *Int. J. Epidemiol.* **43**, 983–988 (2014).
22. T. Goldring, F. Lange, S. Richards-Shubik, "Testing for Changes in the SES-Mortality Gradient When the Distribution of Education Changes Too," National Bureau of Economic Research Working Paper 20993 (2015).
23. A. S. Hendi, *Int. J. Epidemiol.* **44**, 946–955 (2015).
24. A. Aizer, J. Currie, *Science* **344**, 856–861 (2014).
25. D. Brown, A. Kowalski, I. Lurie, "Medicaid as an Investment in Children: What Is the Long-Term Impact on Tax Receipts?" National Bureau of Economic Research Working Paper 20835 (2015).
26. S. Cahodes, S. Kleiner, M. F. Lovenhem, M. Grossman, "Effect of Child Health Insurance Access on Schooling," National Bureau of Economic Research Working Paper 20178 (2014).
27. S. Miller, L. R. Wherry, "The Long-Term Health Effects of Early Life Medicaid Coverage," Social Science Research Network Working Paper 2466691 (2015).
28. L. R. Wherry, B. Meyer, "Saving Teens: Using and Eligibility Discontinuity to Estimate the Effects of Medicaid Eligibility," National Bureau of Economic Research Working Paper 18309 (2013).
29. L. R. Wherry, S. Miller, R. Kaestner, B. D. Meyer, "Childhood Medicaid Coverage and Later Life Health Care Utilization," National Bureau of Economic Research Working Paper 20929 (2015).
30. J. Ludwig, D. L. Miller, *Q. J. Econ.* **122**, 159–208 (2007).
31. H. Hoynes, D. Whitmore-Schanzanbach, D. Almond, "Long Run Impacts of Childhood Access to the Safety Net," National Bureau of Economic Research Working Paper 18535 (2012).
32. A. Isen, M. Rossin-Slater, R. Walker, "Every Breath You Take Every Dollar You'll Make: The Long-Term Consequences of the Clean Air Act of 1970," National Bureau of Economic Research Working Paper 19858 (2014).
33. A. Fenelon, S. H. Preston, *Demography* **49**, 797–818 (2012).
34. D. de Walque, *J. Hum. Resour.* **45**, 682–717 (2010).
35. C. E. Finch, E. M. Crimmins, *Science* **305**, 1736–1739 (2004).

ACKNOWLEDGMENTS

We thank M. Barbieri, A. Case, A. Deaton, J. Goldstein, I. Kuziemko, R. Lee, and K. Wachter, as well as seminar participants at Berkeley, the Chicago Federal Reserve, Fundação Getúlio Vargas São Paulo, Bonn University, University of Munich, Princeton University, ETH Zurich, and the University of Zurich for comments. Supported by Princeton Center for Translational Research on Aging grant 2P30AG024928. Data and code are available at http://dx.doi.org/10.7910/DVN/C2VYNM.

SUPPLEMENTARY MATERIALS

www.sciencemag.org/content/352/6286/708/suppl/DC1
Materials and Methods
Figs. S1 to S8
Tables S1 to S4
References (*36*–*38*)

22 December 2015; accepted 17 March 2016
Published online 21 April 2016
10.1126/science.aaf1437

NEURODEVELOPMENT

Complement and microglia mediate early synapse loss in Alzheimer mouse models

Soyon Hong,[1] Victoria F. Beja-Glasser,[1]* Bianca M. Nfonoyim,[1]* Arnaud Frouin,[1] Shaomin Li,[2] Saranya Ramakrishnan,[1] Katherine M. Merry,[1] Qiaoqiao Shi,[2] Arnon Rosenthal,[3,4,5] Ben A. Barres,[6] Cynthia A. Lemere,[2] Dennis J. Selkoe,[2,7] Beth Stevens[1,8]†

Synapse loss in Alzheimer's disease (AD) correlates with cognitive decline. Involvement of microglia and complement in AD has been attributed to neuroinflammation, prominent late in disease. Here we show in mouse models that complement and microglia mediate synaptic loss early in AD. C1q, the initiating protein of the classical complement cascade, is increased and associated with synapses before overt plaque deposition. Inhibition of C1q, C3, or the microglial complement receptor CR3 reduces the number of phagocytic microglia, as well as the extent of early synapse loss. C1q is necessary for the toxic effects of soluble β-amyloid (Aβ) oligomers on synapses and hippocampal long-term potentiation. Finally, microglia in adult brains engulf synaptic material in a CR3-dependent process when exposed to soluble Aβ oligomers. Together, these findings suggest that the complement-dependent pathway and microglia that prune excess synapses in development are inappropriately activated and mediate synapse loss in AD.

Genome-wide association studies implicate microglia and complement-related pathways in Alzheimer's disease (AD) (*1*). Previous research has demonstrated both beneficial and detrimental roles of complement and microglia in plaque-related neuropathology (*2*, *3*); however, their roles in synapse loss, a major pathological correlate of cognitive decline in AD (*4*), remain to be identified. Emerging research implicates microglia and immune-related mechanisms in brain wiring in the healthy brain (*1*). During development, C1q and C3 localize to synapses and mediate synapse elimination by phagocytic microglia (*5*–*7*). We hypothesized that this normal developmental synaptic pruning pathway is activated early in the AD brain and mediates synapse loss.

The degree of region-specific synapse loss is a stronger correlate of cognitive decline in AD than counts of plaques, tangles, and neuronal loss (*8*, *9*). To determine how early synapse loss occurs, we used superresolution structured illumination microscopy (SIM) (*10*) to quantify synapse density in hippocampal CA1 stratum radiatum of familial AD-mutant human amyloid precursor protein (hAPP) ("J20") transgenic mice (*11*). Quantification of colocalized pre- and postsynaptic puncta [synaptophysin and postsynaptic density 95 (PSD95) (Fig. 1A); synaptotagmin and homer (fig. S1, A to D)] revealed a significant loss of synapses in J20 hippocampus at 3 to 4 months old (mo), an age that precedes plaque deposition (*11*, *12*). Synapse loss in preplaque J20 CA1 was confirmed by electron microscopy (fig. S1G). Confocal imaging also showed synapse loss in CA1, CA3, and dentate gyrus of 3 mo J20 hippocampus but not in striatum (fig. S1E). Synapse

[1]F.M. Kirby Neurobiology Center, Boston Children's Hospital (BCH) and Harvard Medical School (HMS), Boston, MA 02115, USA. [2]Ann Romney Center for Neurologic Diseases, Department of Neurology, Brigham and Women's Hospital (BWH) and HMS, Boston, MA 02115, USA. [3]Alector Inc., 953 Indiana Street, San Francisco, CA 94107, USA. [4]Annexon Biosciences, 280 Utah Avenue Suite 110, South San Francisco, CA 94080, USA. [5]Department of Anatomy, University of California San Francisco (UCSF), San Francisco, CA 94143, USA. [6]Department of Neurobiology, Stanford University School of Medicine, Palo Alto, CA 94305, USA. [7]Prothena Biosciences, Dublin, Ireland. [8]Stanley Center for Psychiatric Research, Broad Institute of MIT and Harvard, Cambridge, MA 02142, USA.
*These authors contributed equally to this work. **†Corresponding author. Email: beth.stevens@childrens.harvard.edu**

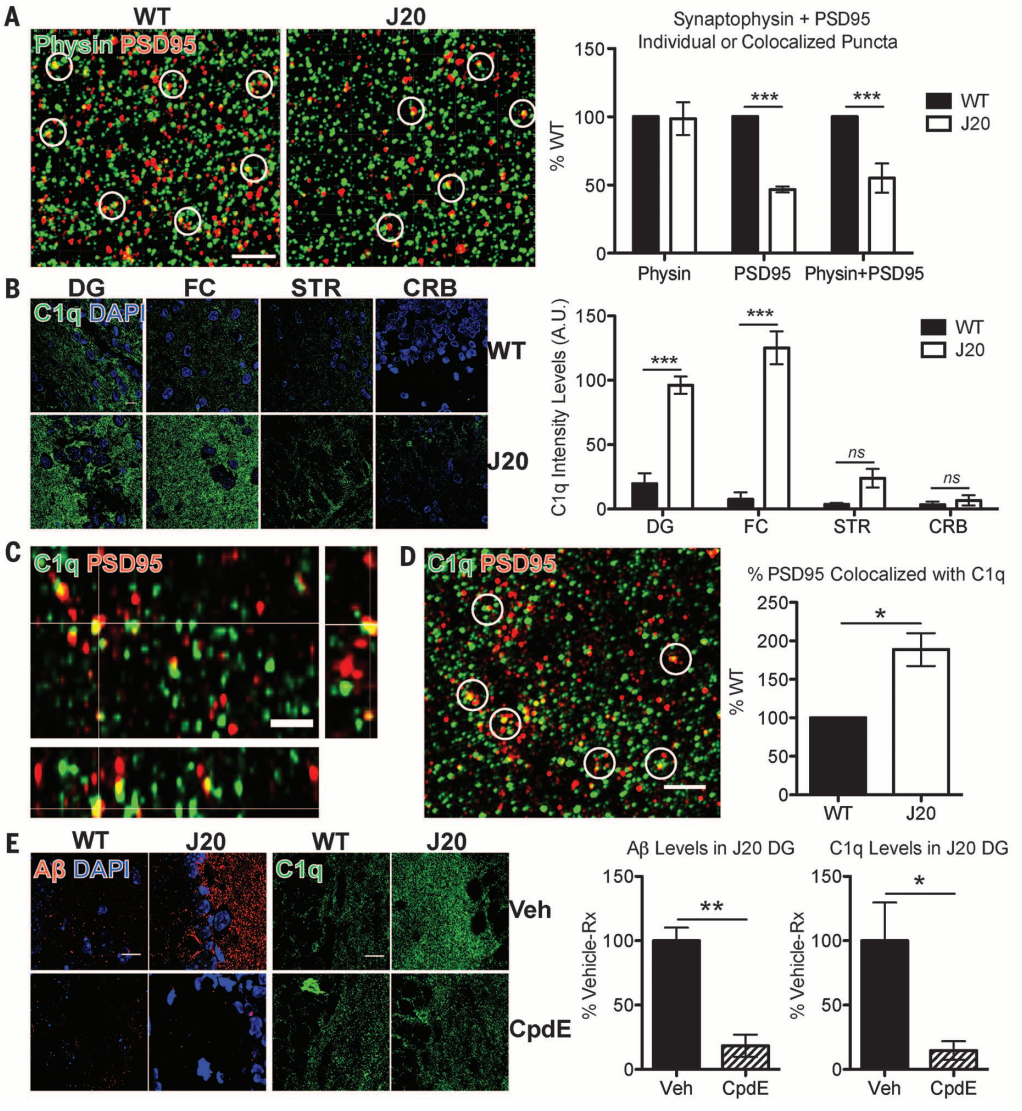

Fig. 1. C1q up-regulation and deposition onto synapses precede preplaque synapse loss in J20 mice. (**A**) Superresolution SIM images of synaptophysin (green)– and PSD95 (red)–immunoreactive puncta in stratum radiatum of 3 mo J20 or WT hippocampus (CA1). Quantification of synaptic puncta or their apposition using Imaris indicates selective loss of PSD95 in J20 hippocampus as compared to their WT littermate controls. See fig. S1. (**B**) Region-specific up-regulation of C1q (green) in 1 mo J20; DG, dentate gyrus; FC, frontal cortex; STR, striatum; CRB, cerebellum; DAPI, 4′,6-diamidino-2-phenylindole. See fig. S2. (**C**) Orthogonal view of SIM image showing colocalization of C1q (green) and PSD95 (red). (**D**) Higher percentage of PSD95 colocalized with C1q in 1 mo J20 dentate gyrus versus WT. (**E**) Compound E reduces deposited soluble Aβ (red) and C1q (green) in 1 mo J20 dentate gyrus, with minimal effect on C1q levels in WT mice. Scale bar, 2 μm (A, C, and D) or 10 μm (B and E). Means ± SEM; $n = 3$ or 4 mice per genotype or per treatment group per genotype. $^{*}P < 0.05$, $^{**}P < 0.01$, or $^{***}P < 0.001$ using two-way analysis of variance (ANOVA) followed by Bonferroni posttest (A and B), two-tailed one-sample t test (D), or two-tailed unpaired t test (E).

levels were not altered in 1 mo J20 brains versus wild-type (WT) littermates (fig. S1F), suggesting that the hippocampal synaptic loss at 3 mo is likely not a result of abnormal synaptic development.

We asked whether the classical complement cascade is up-regulated in preplaque brains when synapses are already vulnerable. C1q immunoreactivity (*13*) (antibody now available at Abcam) was elevated in J20 brains as early as 1 mo and preceding synapse loss (Fig. 1B and fig. S1). C1q elevation was region-specific, particularly in the hippocampus and frontal cortex, two regions vulnerable to synapse loss (*14*) (Fig. 1B and fig. S2A). C1q immunoreactivity was comparable between J20 and WT mice at postnatal day 21 (P21) (fig. S2B), suggesting that elevated levels at 1 mo are likely not a developmental artifact. C1q was also similarly increased in the hippocampus of another model of AD, the APP/PS1 (presenilin 1) mice (*15*) (fig. S2C). Notably, SIM demonstrated colocalization of C1q with PSD95-positive puncta in 1 mo J20 hippocampus (Fig. 1C). A higher percentage of PSD95 colocalized with C1q in the hippocampus of J20 mice than in that of WT littermates (Fig. 1D and fig. S3), suggesting that the C1q-associated synapses may be marked for elimination.

Punctate Aβ was found deposited in J20 hippocampus at 1 mo (fig. S4), long before Aβ plaques deposit (*11*, *12*), raising the question of whether C1q increase in these preplaque brains is dependent on soluble Aβ levels. To test this hypothesis, we injected the mice with compound E, a γ-secretase inhibitor that rapidly decreases Aβ production (*12*). Compound E markedly reduced soluble Aβ levels in J20 mice; there was a corresponding reduction of C1q deposition (Fig. 1E), suggesting that Aβ up-regulates C1q.

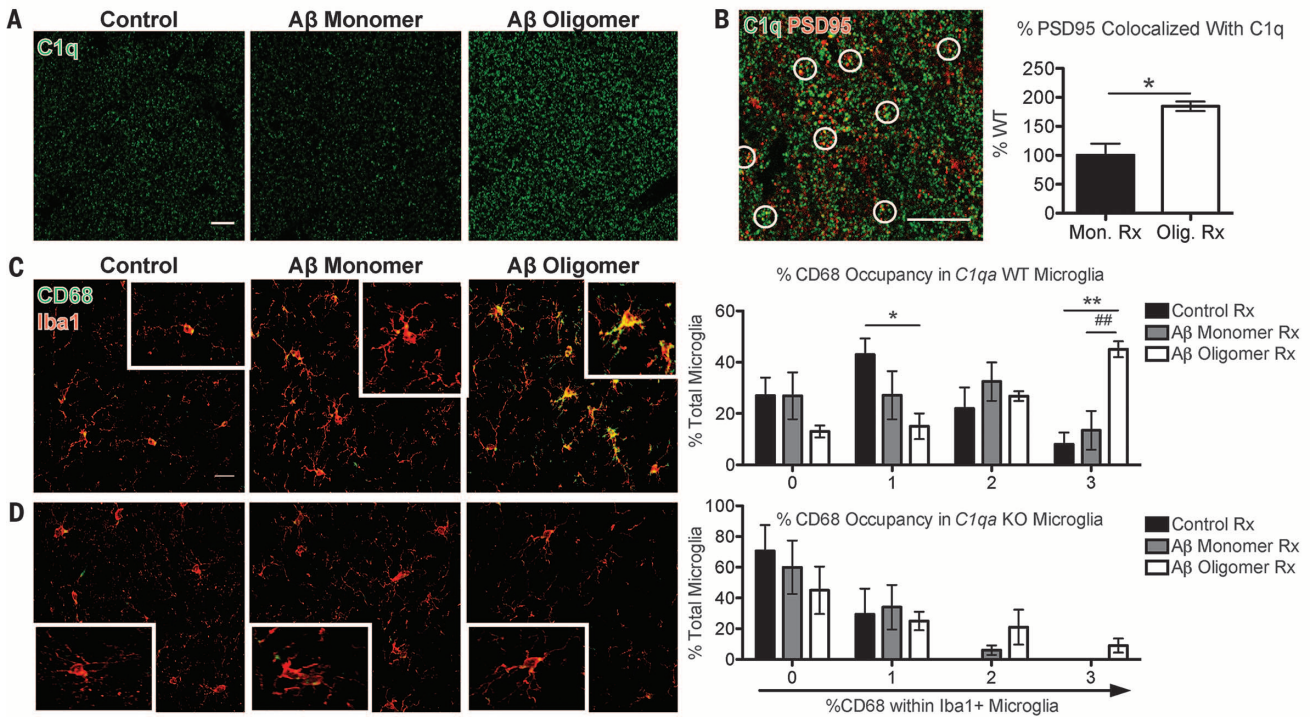

Fig. 2. Oligomeric Aβ increases C1q and microglial phagocytic activity. (**A** and **B**) Soluble Aβ oligomers in WT mice led to elevation of C1q (green) (A) and a higher percentage of PSD95 (red) colocalization with C1q versus monomers (B). (**C** and **D**) oAβ induced high levels of CD68 (green) immunoreactivity in Iba1-positive (red) microglia in WT mice (C), but not in those of *C1qa* KO mice (D). Both had negligible changes in morphology. See fig. S10. Scale bar, 10 μm (A), 5 μm (B), or 20 μm (C). Means ± SEM; n = 3 to 5 mice per treatment group per genotype. $^{*}P < 0.05$ using two-tailed t test (B) or $^{*}P < 0.05$, $^{**}P < 0.01$ versus control-treated or $^{\#\#}P < 0.01$ versus Aβ monomer–treated using two-way ANOVA followed by Bonferroni posttest (C).

Fig. 3. Complement is necessary for synapse loss and dysfunction in AD models. (**A**) Aβ oligomers induced loss of colocalized synapsin- and PSD95-immunoreactive puncta in the contralateral hippocampus of 3 mo WT mice (left panel); however, they failed to do so in *C1qa* KO mice (right panel). (**B**) Coinjection of Aβ oligomers with the function-blocking antibody against C1q, ANX-M1, but not with its IgG isotype control, prevented synapse loss in WT mice. (**C**) Pretreatment of hippocampal slices with the anti-C1q antibody, ANX-M1, prevented Aβ-mediated LTP inhibition (green) versus IgG (red). IgG alone had a minimal effect (blue) versus artificial cerebrospinal fluid (aCSF) vehicle (black). n = 6 to 11 slices per group. (**D**) Percentage of PSD95 co-localized with C3 is increased in APP/PS1 hippocampus versus that of WT mice. (**E** and **F**) Genetic deletion of *C3* prevents synapse loss in 4 mo APP/PS1 mice. Quantification of colocalized immunoreactive puncta for synaptotagmin and homer in dentate gyrus (E) or synaptophysin and PSD95 in CA1 stratum radiatum (F) of WT, APP/PS1, APP/PS1x*C3* KO, and *C3* KO hippocampi. Means ± SEM; n = 3 to 5 mice per genotype or per treatment group per genotype. $^{*}P < 0.05$, $^{**}P < 0.01$, or $^{***}P < 0.001$ using two-tailed one-sample t test (D), one-way (A, C, E, F) or two-way (B) ANOVA followed by Bonferroni posttest. ns, not significant.

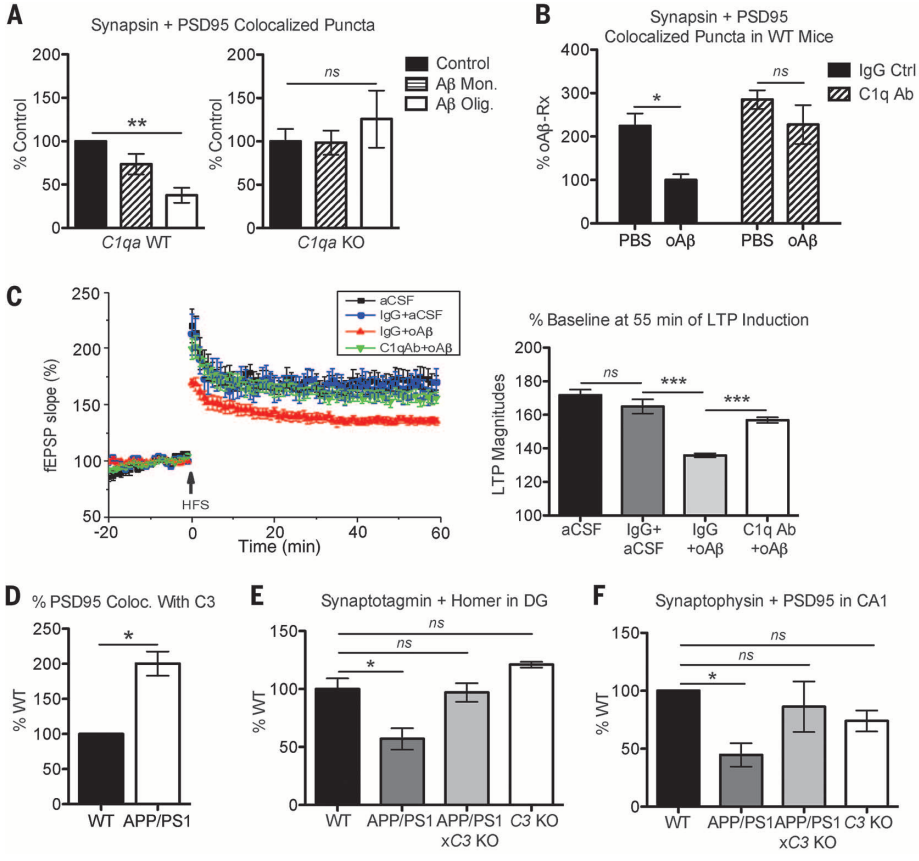

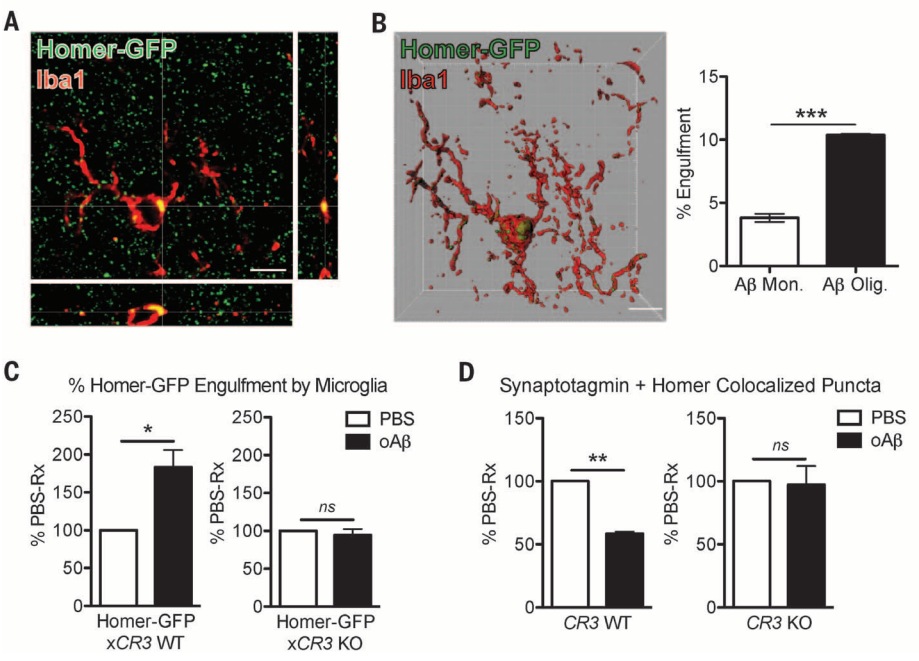

Fig. 4. Microglia engulf synapses via CR3 upon oligomeric Aβ challenge. (**A**) Orthogonal view of high-resolution confocal image shows colocalization of homer-GFP and Iba1 (red). (**B**) Three-dimensional reconstruction and surface rendering using Imaris demonstrate larger volumes of homer-GFP puncta inside microglia of oAβ-injected contralateral hippocampus versus those of monomer-injected. (**C**) Microglia of homer-GFPx*CR3* KO mice (right panel) show less engulfment of homer-GFP when challenged with oAβ versus those of homer-GFP mice (left panel). (**D**) Aβ oligomers failed to induce synapse loss in the contralateral hippocampus of *CR3* KO mice (right panel) as they did in WT mice (left panel). Scale bar, 5 μm (A and B). Means ± SEM; n = 3 mice per treatment group per genotype (n = 6 to 17 microglia analyzed per mouse). *P < 0.05, **P < 0.01, or ***P < 0.0001 using two-tailed t test (B) or two-tailed one-sample t test (C and D). ns, not significant.

To further address whether the increase of C1q is dependent on soluble Aβ, and if so, which species, we injected soluble Aβ oligomers or monomers into lateral ventricles of WT mice. Hippocampus contralateral to the injection site was examined to avoid any surgery-related effects. Oligomeric Aβ (oAβ), which is prefibrillar in nature and acts as a mediator of synapse loss and dysfunction in AD (*4*), but not the relatively innocuous monomeric Aβ or vehicle, induced C1q deposition (Fig. 2A and fig. S5). A higher percentage of PSD95 colocalized with C1q in oAβ-injected versus monomer-injected mice (Fig. 2B), in a manner similar to this colocalization in J20 mice. Together, these findings show an early and aberrant increase and synaptic localization of C1q in multiple AD model systems. Furthermore, fluorescent in situ hybridization (FISH) demonstrated up-regulated *C1qa* expression in microglia (fig. S6), implicating microglia as a major source of C1q in these preplaque brains.

To test whether C1q and oAβ act in a common pathway to eliminate synapses, we injected oAβ into lateral ventricles of *C1qa* knockout (KO) mice (*16*). Soluble oAβ induced a significant loss of colocalized synapsin- and PSD95-immunoreactive puncta in WT mice within 72 hours (Fig. 3A, left panel) (*17*). In contrast, oAβ failed to induce synapse loss in *C1qa* KO mice (Fig. 3A, right panel), suggesting that C1q is required for oAβ-induced synapse loss in vivo. To determine whether local, acute inhibition of C1 activation could similarly blunt the synaptotoxic effects of oAβ, we used an antibody against C1q (anti-C1q) (ANX-M1, Annexon Biosciences), which blocks the classical complement cascade (see fig. S7 and supplementary methods). Coadministration of the ANX-M1 anti-C1q antibody, but not its immunoglobulin G (IgG) isotype control, prevented oAβ from inducing synapse loss in WT mice (Fig. 3B). Thus, blocking C1 activation by either genetic or antibody-mediated means lessened oAβ's synaptotoxic effects.

To determine whether C1q is associated with synaptic dysfunction, we asked whether the established ability of oAβ to potently inhibit long-term potentiation (LTP) (*4*) was dependent on C1q. We tested the functional effects of the ANX-M1 anti-C1q antibody in acute hippocampal slices treated with oAβ. IgG alone had negligible effects on LTP induction in WT mouse hippocampal slices and on the ability of oAβ to inhibit LTP; however, pretreatment of hippocampal slices with the anti-C1q antibody significantly prevented the impairment of LTP by oAβ (Fig. 3C). Neither ANX-M1 nor its IgG control altered basal synaptic neurotransmission (fig. S8). Collectively, these results in hippocampal slices and in mice support C1q as a key mediator of oAβ-induced synaptic loss and dysfunction.

In the healthy developing brain, C1q promotes activation of C3, which opsonizes subsets of synapses for elimination, a process that is down-regulated in the mature brain (*5*, *6*). However, oAβ induced a significant C3 deposition in WT adult mice (fig. S7A, upper panel). This was significantly reduced in both the *C1qa* KO (fig. S7A, lower panel) and the ANX-M1 anti-C1q antibody–treated WT mice (fig. S7B), suggesting that the C3 deposition in this model is downstream of the classical complement cascade. Consistent with these findings, a higher percentage of PSD95 colocalized with C3 in J20 and APP/PS1 brains (Fig. 3D and fig. S9). To determine whether C3 is necessary for early synapse loss in AD genetic models, we crossed APP/PS1 mice, which, similar to the J20 mice, had a significant increase and localization of C1q and C3 onto hippocampal synapses (figs. S2C and S9), to *C3*-deficient mice (*18*). Quantification of colocalized pre- and postsynaptic puncta demonstrated synapse loss in 4 mo APP/PS1 hippocampus as compared to WT; however, APP/PS1x*C3* KO mice did not display this synapse loss (Fig. 3, E and F). Together, our data indicate that genetic deletion of *C3* ameliorates synapse loss in APP/PS1 mice, providing further evidence that the classical complement cascade mediates early synapse loss in AD mouse models.

Microglia express complement receptors and mediate synaptic pruning in the developing brain (*1*, *6*), raising the question of whether this normal developmental pruning pathway could be activated to mediate synapse loss in the preplaque AD brain. Consistent with this hypothesis, microglia had increased amounts of the lysosomal protein CD68 in J20 hippocampus compared to WT and less so in striatum, a less vulnerable region (figs. S1C and S10). Furthermore, in WT mice challenged with oAβ, microglia had significantly increased levels of CD68 immunoreactivity (Fig. 2C). However, in *C1qa* KO mice in which synapse loss was rescued, oAβ failed to induce such an increase (Fig. 2D), suggesting that microglia eliminate synapses through the complement pathway.

To directly test whether phagocytic microglia engulf synaptic elements, we adapted our in vivo synaptic engulfment assay (*19*) using intracerebroventricular injections of Aβ in homer-GFP (green fluorescent protein) mice (*20*) (Fig. 4A). oAβ induced a significantly higher volume of internalized homer-GFP in microglia than monomeric Aβ controls did at the contralateral hippocampus (Fig. 4B), indicating that microglia engulf synaptic elements when challenged with oAβ. Internalized homer-GFP often colocalized

with CD68 (fig. S11A), suggesting that the engulfed synapses are internalized into lysosomal compartments in a manner similar to that of developmental synaptic pruning (*6*). Notably, oAβ failed to increase synaptic engulfment in microglia lacking CR3 (*21*), a high-affinity receptor for C3 expressed on macrophages [homer-GFPx*CR3* KO versus homer-GFP mice, which received tail vein injections of phosphate-buffered saline (PBS) or oAβ (Fig. 4C)]. These data demonstrate that CR3 is necessary for oAβ-dependent engulfment of synapses by microglia.

To test whether inhibition in microglial engulfment leads to protection against oAβ-induced synapse loss, we performed tail vein injections of oAβ into WT and *CR3* KO mice. oAβ induced synapse loss in the hippocampus of WT mice but not in that of *CR3* KO mice (Fig. 4D). All CR3-positive microglia were P2RY12-positive (fig. S11), indicating that they are resident cells (*22*). Altogether, these results suggest that resident microglia engulf synaptic material when challenged by oAβ through a complement-dependent mechanism.

Synaptic deficits occur in early AD and mild cognitive impairment before onset of plaques and are some of the first signs of the neuronal degenerative process (*4*, *23*–*25*). Here we identify critical synaptotoxic roles of complement and microglia in AD models before plaque formation and neuroinflammation, in regions of the hippocampus undergoing synapse loss. Using multiple experimental approaches, we demonstrate a region-specific increase of phagocytic microglia and accumulation of C1q and C3 on synapses in preplaque brains. Microglia in the adult brain, when challenged with synaptotoxic, soluble Aβ oligomers, engulf synapses in the absence of plaque aggregates; deletion of CR3 blocks this process. Finally, inhibiting C1q, C3, or CR3 activity rescues synaptic loss and dysfunction.

Our data suggest a local activation of a developmental pruning pathway (*5*, *6*) as a key mechanism underlying oAβ-induced synapse loss in preplaque AD brain. C1q is aberrantly increased by diffusible oAβ in a region-specific manner and deposits onto synapses, triggering the activation of downstream classical complement pathway and phagocytic microglia. Blocking Aβ production in J20 mice significantly ameliorated C1q deposition in the hippocampus, and genetic or antibody-mediated inhibition of complement blocks oAβ from inducing microglial synaptic engulfment, synapse loss, and LTP inhibition. These complementary findings have direct therapeutic relevance.

We propose a model in which C1q and oAβ operate in a common pathway to activate the complement cascade and drive synapse elimination by microglia through CR3 (fig. S12). This could occur in multiple ways: Soluble oAβ associates with synaptic membranes and other synaptic markers (*4*, *26*); thus, oAβ bound to synapses may anchor C1q directly. Alternatively, oAβ binding to synapses may weaken the synapse (*4*) and expose a C1q receptor. Although specific receptors for C1q at synapses are not yet known, we have shown that C1q binds synapses in vulnerable regions undergoing synapse loss (*5*, *27*). It is also plausible that oAβ and C1q may work indirectly to mediate synapse loss through cytokines such as transforming growth factor–β (*7*), through microglial or astrocytic activation, or through other mechanisms, including major histocompatibility complex class I (MHCI)–PirB, another immune pathway critical for synapse elimination in development and AD (*28*–*30*).

Finally, our studies show that resident microglia in the adult central nervous system phagocytose synapses when challenged by synaptotoxic oAβ, implicating microglia as potential cellular mediators of synapse loss. Although microglia and complement activation are prominently involved in plaque maintenance and related periplaque neuropathology, their roles have heretofore been largely regarded as a secondary event related to neuroinflammation (*2*). Our studies directly challenge this view and suggest that microglia and immune-related pathways can act as early mediators of synapse loss and dysfunction that occur in AD models before plaques form. Although the complement pathway may not be involved in all pathological routes to AD, including plaque-associated synapse loss, the work reported here provides new insights into how synapses are lost in AD. It will be important in future studies to examine whether this microglia or the complement-dependent pathway also plays a role in plaque-associated synapse loss or in other synaptopathies, including tauopathies and Huntington's disease. If so, our findings may suggest complement and microglia as potential early therapeutic targets in AD and other neurodegenerative diseases involving synaptic dysfunction and memory decline.

REFERENCES AND NOTES

1. S. Hong, L. Dissing-Olesen, B. Stevens, *Curr. Opin. Neurobiol.* **36**, 128–134 (2016).
2. T. Wyss-Coray, J. Rogers, *Cold Spring Harb. Perspect. Med.* **2**, a006346 (2012).
3. M. E. Benoit *et al*., *J. Biol. Chem.* **288**, 654–665 (2013).
4. L. Mucke, D. J. Selkoe, *Cold Spring Harb. Perspect. Med.* **2**, a006338 (2012).
5. B. Stevens *et al*., *Cell* **131**, 1164–1178 (2007).
6. D. P. Schafer *et al*., *Neuron* **74**, 691–705 (2012).
7. A. R. Bialas, B. Stevens, *Nat. Neurosci.* **16**, 1773–1782 (2013).
8. S. T. DeKosky, S. W. Scheff, *Ann. Neurol.* **27**, 457–464 (1990).
9. R. D. Terry *et al*., *Ann. Neurol.* **30**, 572–580 (1991).
10. S. Hong, D. Wilton, B. Stevens, D. S. Richardson, Structured Illumination Microscopy for the investigation of synaptic structure and function. *Methods in Molecular Biology; Synapse Development: Methods and Protocols*.
11. L. Mucke *et al*., *J. Neurosci.* **20**, 4050–4058 (2000).
12. S. Hong *et al*., *J. Neurosci.* **31**, 15861–15869 (2011).
13. A. H. Stephan *et al*., *J. Neurosci.* **33**, 13460–13474 (2013).
14. J. A. Harris *et al*., *J. Neurosci.* **30**, 372–381 (2010).
15. J. L. Jankowsky *et al*., *Hum. Mol. Genet.* **13**, 159–170 (2004).
16. M. Botto *et al*., *Nat. Genet.* **19**, 56–59 (1998).
17. D. B. Freir *et al*., *Neurobiol. Aging* **32**, 2211–2218 (2011).
18. M. R. Wessels *et al*., *Proc. Natl. Acad. Sci. U.S.A.* **92**, 11490–11494 (1995).
19. D. P. Schafer, E. K. Lehrman, C. T. Heller, B. Stevens, *J. Vis. Exp.* **88**, 51482 (2014).
20. T. Ebihara, I. Kawabata, S. Usui, K. Sobue, S. Okabe, *J. Neurosci.* **23**, 2170–2181 (2003).
21. A. Coxon *et al*., *Immunity* **5**, 653–666 (1996).
22. O. Butovsky *et al*., *Nat. Neurosci.* **17**, 131–143 (2014).
23. D. J. Selkoe, *Science* **298**, 789–791 (2002).
24. S. W. Scheff, D. A. Price, F. A. Schmitt, E. J. Mufson, *Neurobiol. Aging* **27**, 1372–1384 (2006).
25. S. W. Scheff, D. A. Price, F. A. Schmitt, S. T. DeKosky, E. J. Mufson, *Neurology* **68**, 1501–1508 (2007).
26. S. Hong *et al*., *Neuron* **82**, 308–319 (2014).
27. A. H. Stephan, B. A. Barres, B. Stevens, *Annu. Rev. Neurosci.* **35**, 369–389 (2012).
28. A. Datwani *et al*., *Neuron* **64**, 463–470 (2009).
29. T. Kim *et al*., *Science* **341**, 1399–1404 (2013).
30. H. Lee *et al*., *Nature* **509**, 195–200 (2014).

ACKNOWLEDGMENTS

We thank B. Sabatini (HMS), T. Bartels (BWH), and members of the Stevens laboratory for critical reading of the manuscript; L. Dissing-Olesen (BCH) for help with the conceptual figure (fig. S12), M. Ericsson [HMS electron microscopy (EM) facility] for EM imaging, K. Kapur (BCH) for advice on statistics, D. M. Walsh (BWH) for Aβ oligomers (S26C), S. Okabe (University of Tokyo) for homer-GFP mice, and M. Leviten and T. Yednock (Annexon Biosciences) for characterization and advice on the ANX-M1 anti-C1q antibody; D. Richardson (Harvard Center for Biological Imaging), A. Hill BCH Intellectual and Developmental Disabilities Research Center Cellular Imaging Core NIH-P30-HD-18655, and H. Elliot and T. Xie (HMS Image and Data Analysis Core) for assistance with imaging and data analysis; and S. Kim (BWH), K. Colodner (BCH), and S. Matousek (BWH) for assistance with mice. The J20 mice, *C1qa* KO mice, P2RY12 antibody, and the ANX-M1 C1q function-blocking antibody are available from L. Mucke, M. Botto, O. Butovsky, and A. Rosenthal under material transfer agreements with UCSF Gladstone, Imperial College London, BWH, and Annexon Biosciences, respectively. A.R. is a cofounder, consultant, and chairman of the board of directors; B.A.B. is a cofounder and chairman of the scientific advisory board; and B.S. serves on the scientific advisory board of Annexon LLC. A.R., B.A.B., and B.S. are minor shareholders of Annexon LLC. All other authors declare no competing financial interests related to this project. The following patents related to this project have been granted or applied for: PCT/2015/010288 (S.H. and B.S.), US14/988387 and EP14822330 (S.H., A.R., and B.S.), and US8148330, US9149444, US20150368324, US20150368325, US20150368326, and US20120328601 (B.S. and B.A.B.). This work was funded by an Edward R. and Anne G. Lefler Fellowship (S.H.), Coins for Alzheimer's Research Trust (B.S.), Fidelity Biosciences Research Initiative (F-Prime) (B.S. and C.A.L.), JPB Foundation (B.A.B.), the National Institutes of Health AG000222 (S.H.), National Institute of Neurological Disorders and Stroke–NIH R01NS083845 (D.J.S.), National Institute on Aging–NIH 1RF1AG051496A (B.S.). Supplementary materials contain additional data, including materials and methods. S.H. and B.S. designed the study and wrote the manuscript, with help from all authors. S.H. performed most experiments and data analysis; V.F.B.-G. and B.M.N. performed microglial activation and engulfment experiments along with immunohistochemistry; S.R. and K.M.M. performed C1q immunohistochemistry; A.F. performed FISH; S.L. performed electrophysiology; Q.S. and C.A.L. assisted with design and collection of APP/PS1 tissue; A.R. and B.A.B. designed and characterized the ANX-M1 anti-C1q antibody; and D.J.S. contributed in the discussions and experimental design.

SUPPLEMENTARY MATERIALS

www.sciencemag.org/content/352/6286/712/suppl/DC1
Materials and Methods
Figs. S1 to S12

10 November 2015; accepted 18 March 2016
Published online 31 March 2016
10.1126/science.aad8373